Nanopages 7 (2012), 17–24
DOI: 10.1556/Nano.2010.00003

Development and experiments with conductive oxide nanofilm coated planar waveguide sensors

I. Szendrő[1], K. Erdélyi[1], Zs. Puskás[2], M. Fábián[1], N. Adányi[3] and K. Somogyi[1]

[1]MicroVacuum Ltd., Kerékgyártó u. 10, H-1147 Budapest, Hungary
[2]Minvasive Ltd., Goldmann Gy. tér 3, H-1111 Budapest, Hungary
[3]Central Food Research Institute, H-1537 Budapest, P.O. Box 393, Hungary

Abstract. Due to the changes of the refractive indices, the planar optical waveguides are sensitive to the surrounding media, to the adsorbates, etc. on their surface. The sensitivity of such a waveguide layer can be enhanced when its thickness is lowered down to the nanometer range. Such sensors can be successfully operated both in inorganic chemistry and in life sciences as label free biosensors. Principles and some results are demonstrated. Further on, application of transparent conductive oxides for voltammetric measurements in combination with the classical waveguide sensor will be demonstrated. Development and results of a combined system is described and first results with simultaneous measurements are demonstrated. An indium tin oxide nanolayer is deposited and activated on the top of the sensor chip. This electrically conductive oxide layer serves as working electrode in the specially developed electrochemical cuvette. In this work results are presented for simultaneous use of these two methods and for simultaneous measurement of refractive index changes of the waveguiding system and that of electrical current changes. The first basic results are demonstrated using H_2O_2 and dye solutions, using KCl and TRIS as buffer and transport media.

Keywords: lightmode spectroscopy, electrochemistry, microbiology, planar optical waveguides, transparent conductive oxides, indium tin oxide

PACS: 61.46.Hk, 73.61.Le, 81.05-t, 81.05.Je.

Introduction

The basic elements of integrated optics were developed in the early 1970s, since thin film technology was widely used in electronics already. It was found that a thin transparent dielectric film, with refractive index higher than that of the neighbouring contacting media, is a good optical waveguide. It also became clear that the waveguide modes are very sensitive to the interfacial and surfacial conditions.

Due to the changes of the refractive indices, optical waveguides are normally sensitive to the various inhomogeneities inside the waveguide, to the surrounding media and also to the surface contaminations. Various sensor systems were developed based on this principle. One of the most sensitive and effective systems is the optical waveguide lightmode spectroscopy (OWLS). One of the main problems is the incoupling of the light into the waveguide. Our OWLS sensor chips contain a Bragg-like grating for incoupling of the incident laser beam into the waveguide layer. This basic waveguide layer can be covered with various further solid layers in order to sensitise the chip for selected specific applications, e.g. also for label free microbiological investigations.

The incoupling occurs at well-defined incident angles [1]. The evanescent field of the incoupled light detects the surface coating and the incoupling angles will indicate the influence of the surface conditions. Such optical waveguide lightmode sensors were developed on the basis of transparent $Si_xTi_{1-x}O_2$ layers with the necessary grating [2, 3]. Depending on the amount and polarizability of any surfacial (e.g. adsorbed) layers, the electric and magnetic modes of the light are reflected with a certain phase-shift. Due to the phase-shift, the

Unauthenticated | Downloaded 06/25/24 06:06 PM UTC

light intensity of both the electric (TE) and magnetic (TM) fields attain each a maximum at certain, but different angles (just the incoupling angles) between the normal of the chip and the incident direction of the laser beam. The incoupling angles α(TE) and α(TM) for electric and magnetic modes are evaluated from the measured spectra. The effective refractive indices N(TE) and N(TM) of the waveguide structure are calculated on the basis of incoupling angles. Furthermore, on this basis, using the N(TE) and N(TM) values, the OWLS method allows not only qualitative, but also quantitative evaluation of the mass of adsorbed species, including also biological ones [1–5].

Independent of the optical methods, electrochemical methods are also widely used both in inorganic and organic chemistry, and also advantages in microbiology were demonstrated. Since both voltammetric and/or potentiometric electrochemical measurements and the OWLS method also play paramount importance in the same and similar investigations, presently the need of the combination of the lightmode spectroscopy and voltammetric methods is of vital importance. However, the $Si_xTi_{1-x}O_2$ waveguide layer is a dielectric layer and the electrochemical measurements require a conducting electrode. Thus, optically transparent, but electrically conductive thin layer must be deposited on the grated OWLS sensor.

In this work results of efforts and developments are presented for the integration of these two methods and for simultaneous measurement of refractive index changes of the waveguiding system and that of the electrical current changes due to the reactions of the cells/molecules/ions to be investigated.

Experimental details and results

Like several planar optical devices, such as displays of various kinds, solar cells, light emitting devices, surface sensors, thermally insulating windows etc., the electrochemical OWLS system also require transparent *conductive* thin planar oxide layer. Though these are contradicting requirements in some extent, a combination of transparency and electrical conduction can be achieved in different types of materials. Thus, investigation of various compositions and that of their relevant properties has an increasing importance in general [e.g. 7 to 10].

A 50% transmittance can be achieved depositing extremely thin conducting metallic layers, but in our case the application of such coatings was not approved. Another layer category can be found among the wide bandgap metal-oxide layers. It was reported earlier that good electrical conductivity and high optical transparency can co-exist. Though there is a great variety of alternative binary and ternary oxides, the combination of SnO_2 and In_2O_3 (or Sn doped indium oxide), called as indium tin oxide (ITO) achieved the greatest success both in preparation/deposition technology and application [11]. Nevertheless the theoretical understanding of the electronic structure, especially defect chemistry and carrier generation processes remained very limited [12].

Our OWLS technique is based on the measurement of the incident angle dependent photocurrent spectra of a linearly polarized laser beam (He-Ne laser, 632.8 nm) directed to the surface grating of the sensor chip. The glass substrate based chip is covered by a thin waveguide layer (SiO_2–TiO_2) deposited by sol-gel method and the diffraction grating is formed on the top of this layer. This oxide layer shows excellent optical transparency and stability, but it is a good dielectric.

The electrochemical application needs, however, an electrically conductive layer. For these purposes basically ITO nanolayer coated chips were further developed (see Fig. 1). Ten nm thick ITO layers were deposited by evaporation. A post growth annealing at 500 °C

Unauthenticated | Downloaded 06/25/24 06:06 PM UTC

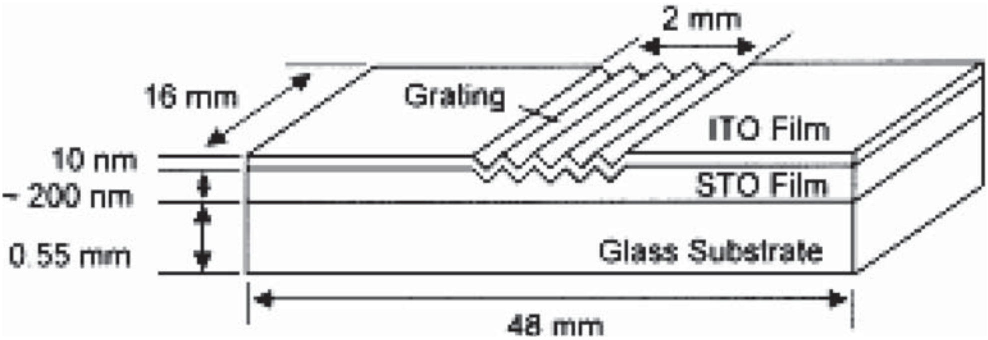

Fig. 1. Schema of the coated optical waveguide lightmode spectroscopy sensors.
The basic standard chip coated with a thin transparent and electrically conducting ITO layer

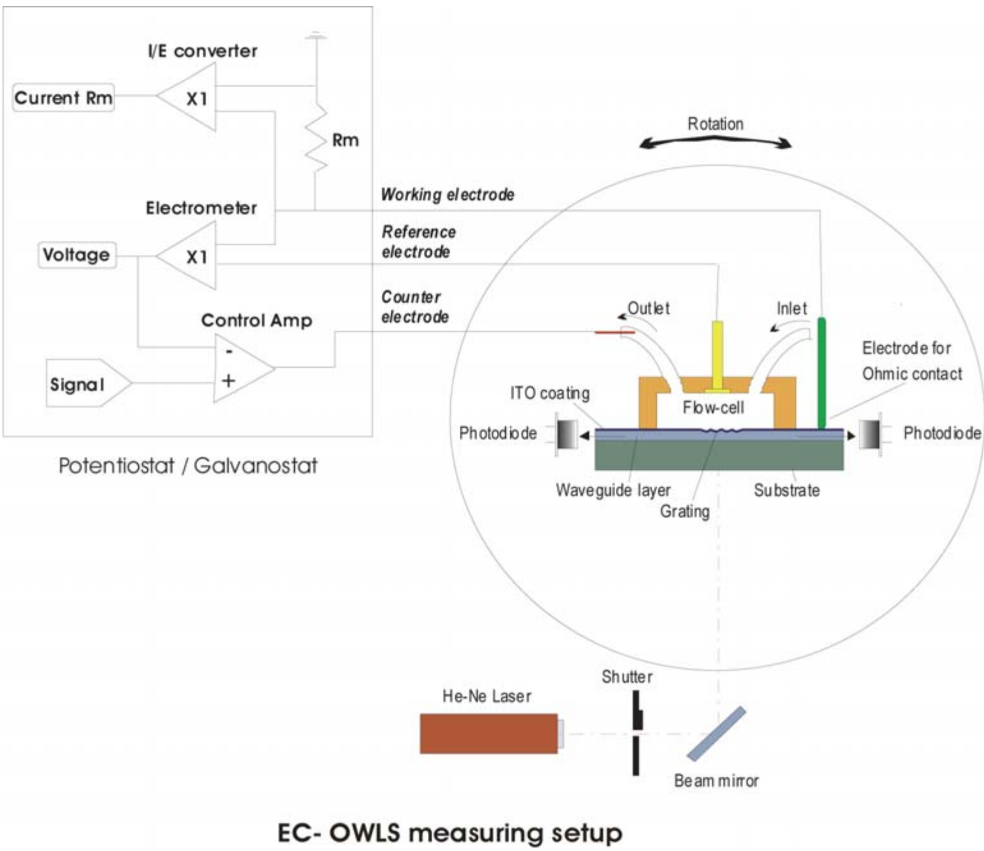

Fig. 2. The schematic of the setup for the integration of lightmode spectroscopy and voltammetric measurements

in O_2 ambient for 3 hours ensures the properties required in electrical measurements. These layers show sufficiently good n-type electrical conductivity and their good optical transparency corresponds to the requirements of the OWLS. This electrically conductive oxide layer serves as working electrode in the specially developed electrochemical cuvette. Outstanding

Unauthenticated | Downloaded 06/25/24 06:06 PM UTC

sensibility of the position of OWLS peaks on any modifications attempting the surface allows the successful application of these layers.

The main goal, however, is that the presence of the electrical field in an electrochemical (EC) cuvette incorporated into an OWLS measuring instrument affects both the transport and the adsorption/desorption processes of the investigated species at the surface of the sensor [4, 6]. An integrated EC-OWLS measuring system was developed according to this. Figure 2 shows schematically the setup. The EC cuvette is shown in the circle and shows the path of the EC solutions, the position of the counter and reference electrodes. The working electrode is the ITO layer covering the basic OWLS sensor chip (Fig. 1). The principle of the light incoupling method and the measurement of the angle dependence of the photocurrent, and also the principles of the electrochemical measuring system can be followed in Fig. 2. In this system short-time injecting of the solute of the species to be investigated can be performed during the continuous flow of a buffer solution (this technical part is not shown in the figure).

In practice, there are two main electrochemical manoeuvres for the investigation of the effects of the electrical field in an electrolyte. One of them is the chrono voltammetric approach, a second one is the cyclic voltammetry. Both of them have different variations. Here we demonstrate examples of both of them which were used, partly, for calibration purposes. The changes of the position of incoupling angles and those of the effective refractive indices due to the base solutions are clearly seen, due to the injection of species to be studied and also on the applied potential.

Figure 3 shows changes of the incoupling angles with various conditions. Two basic stabilizer solutions were used: TRIS and KCl, which are commonly used both in biology and in electrochemistry. H_2O_2 was used for injections in three different concentrations: 10^{-5}, 10^{-4} and 10^{-3} v/v % and each of these solutions were injected three times consecutively into the main buffer stream. It was expected that the stabilizing current of the EC system will indicate the appearance of the injected dopant. A 0.6 V constant potential was applied for the measurements. The current between the working (ITO) and counter (Pt) electrodes was measured. According to the main aim, angle dependent photocurrent spectra and the electrical parameters were measured simultaneously. The difference in the effect of the buffer solution is indicated only on the inset in Fig. 3a, otherwise figures show the effect of H_2O_2 injection using KCl buffer solution. It is seen that in this combination of various parameters the sensitivity in H_2O_2 is at about 10^{-5} v/v %! Incoupling angle changes in both modes correspond to the presence of H_2O_2 (Fig. 3b). The height of the current peaks corresponds to the concentration of the H_2O_2 solution. The inset in Figure 3a demonstrates that the sensibility of the measurement is better, when KCl solution is used as buffer, since the electrical conductivity of KCl is greater (height of the peaks, inset in Fig. 3a).

Application of a slow triangle voltage ramp of the potential is common in electrochemical investigations. Figure 4 and Fig. 5 demonstrate the effects of this cyclic voltammetry in the EC-OWLS system, using toluidine blue dye solution. In Fig. 4 five cycles of the voltage and current dependences are shown. In Fig. 5 the usual view of the hysteresis curves of cyclic voltammetry are shown at different flow rates and at different voltage steps. The shape of the hysteresis is fully corresponds to the specificity of the toluidine blue labelling solution.

The shift of the angle dependent photocurrent peaks allows not only the determination of the effective refractive index of the waveguide system and further calculations lead to the determination of the refractive index of the covering media/species and also the mass of these adsorbed species [3–5, 13, 14]. Figure 6 shows the change of the mass of organic spe-

Unauthenticated | Downloaded 06/25/24 06:06 PM UTC

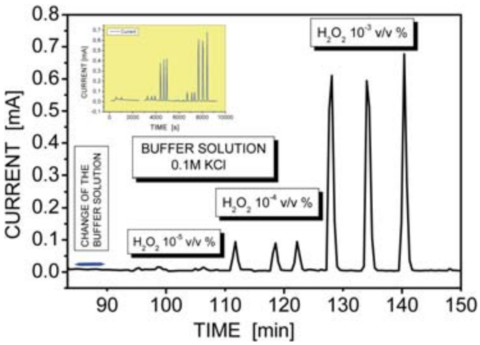

Fig. 3a. Time-dependence of the anodic current. The peaks correspond to the moments of injection of H_2O_2 solutions. The inset shows the time dependence in a wider range, including also all peaks produced by the H_2O_2 injections when using TRIS solution first. The moment of the change of the buffer solutions (from TRIS to KCl) is also indicated at about 5000 s

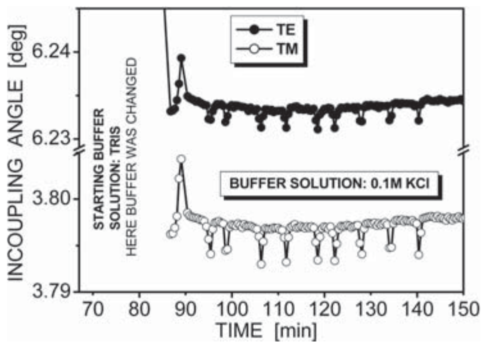

Fig. 3b. Time dependence of the incoupling angle positions of the photocurrent peaks for the magnetic (TM) and electric (TE) modes, when H_2O_2 was injected into the system

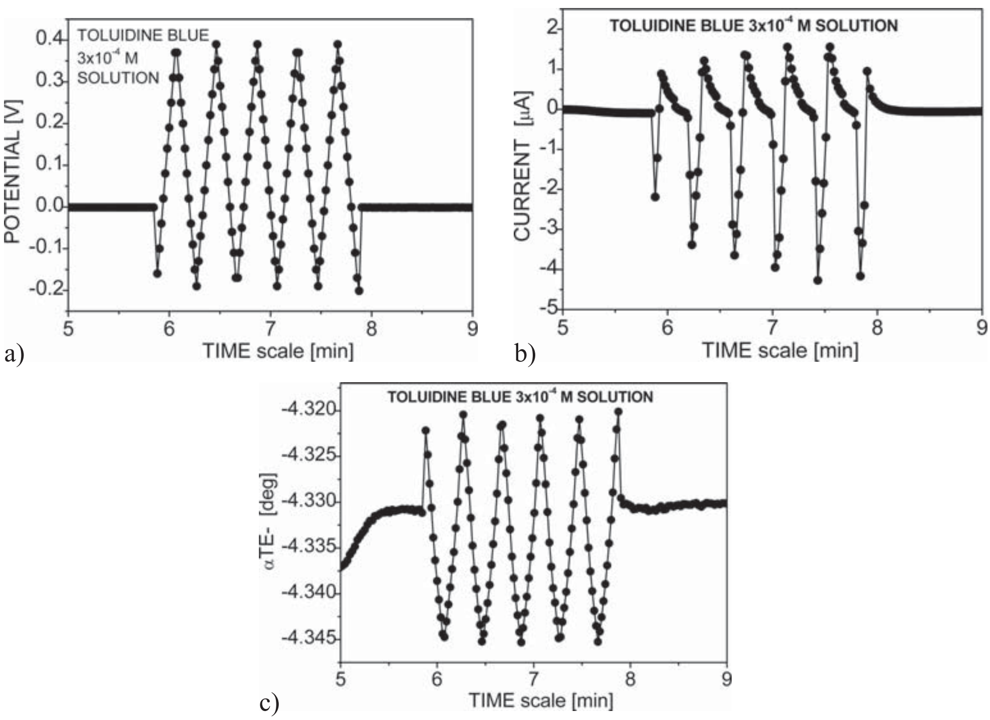

Fig. 4. Slow cyclic voltammetric experiment with toluidine blue solution in TRIS. Five triangular ramps were applied. All data are shown in real time dependence of the process. a) the ramp type changes of the applied potential; b) the current changes with potential variation; c) the incoupling angle position dependence of the electric mode of the light on the applied varying potential

Unauthenticated | Downloaded 06/25/24 06:06 PM UTC

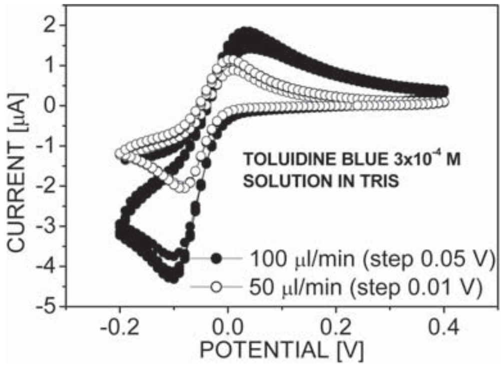

Fig. 5. The characteristic hysteresis of the toluidine blue measured between –0.2 and +0.4 V

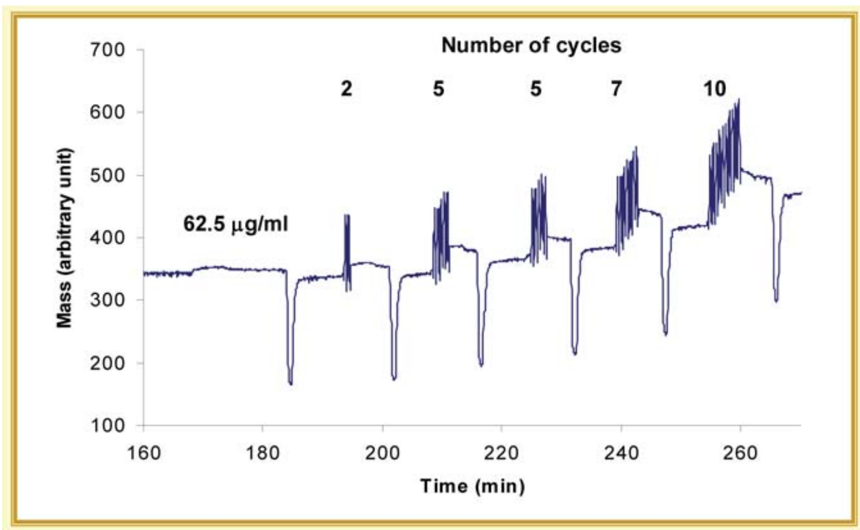

Fig. 6. The change of the mass of organic species deposited and released (oxidation and reduction processes) on the ITO surface in EC-OWLS system with long range, repetitive cyclic voltammetric measurements in the case of variamine solution

cies deposited and released (oxidation and reduction processes) on the ITO surface in EC-OWLS system with long range, repetitive cyclic voltammetric measurements (see also Fig. 4b for the shape of the angle dependence). The increase of the deposited mass with the increasing number of depositing cycles is demonstrated.

The Fig. 7 shows some results of application of EC-OWLS in direct microbiological experiments. *Escherichia coli* bacteria were studied in respect of their survival due to the surrounding temperature. The reaction of living and dead cells is different to the polarisation voltage. This way the mass of the immobilised cells and the ratio of living and immobilised cells were determined.

Unauthenticated | Downloaded 06/25/24 06:06 PM UTC

a)
b)

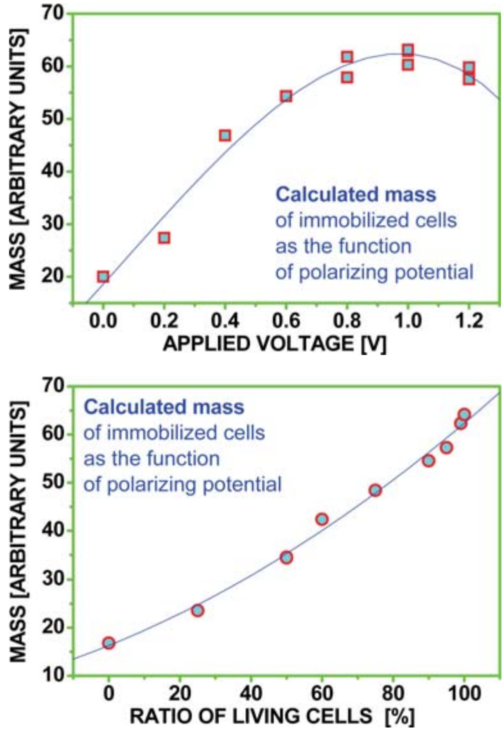

Fig. 7. Determination of the mass of living and immobilised *Escherichia coli* bacteria in dependence of the applied voltage.
a) mass signal on the ITO working electrode of the living cells;
b) the ratio of the living and immobilised bacteria (the same voltage values as in Fig. 7a).

Conclusions

Development in label free methods of microbiology suggested the needs in more complex and more sensitive methods. Here a method was successfully developed with the combination of a label free optical surface sensor and voltammetric methods. This approach proved its applicability both in chemistry and life sciences. Microbiological experiments demonstrated the unique possibilities of this method and the behaviour of the ITO layers during the measurements (cleaning after each measurement, washing in various solvents, acids and water soluble chemicals) was also inspected. It was observed that the high quality ITO nanolayers withstand several operations. This way a stable, biologically applicable layer can be formed and regenerable sensors can be produced and calibrated using ITO layers with 10 nm (or less) thickness.

Acknowledgment

This work was partly supported by EU NATCO project (FP6-511925).

Unauthenticated | Downloaded 06/25/24 06:06 PM UTC

References

[1] W. Lukosz, *Sensors and Actuators* **B 29,** 37–42 (1995).
[2] J. J. Ramsden, *J. Molecular Recognition* **10,** 109–120 (1997).
[3] K. Erdélyi, A. G. Frutos, J. J. Ramsden, I. Szendrő, G. Voirin, "Grating Based Optical Biosensors," in *Handbook of Biosensors and Biochips,* edited by R. Marks, C. H. Lowe, D. Cullen, H. Weetall and I. Karube: John Wiley and Sons, in press.
[4] J. Vörös, J. J. Ramsden, G. Csucs, I. Szendrő, *Biomaterials* **23,** 3699–3710 (2002).
[5] J. P. Bearinger, J. Vörös, J. A. Hubbel, M. Textor, *Biotechnol. Bioeng.* **82,** 465–469 (2003).
[6] J. Domaradzki, A. Borkowska, D. Kaczmarek, E. Prociow, *J. Non-Crystalline Solids* **352,** 2324–2326 (2006).
[7] D. C. Look, B. Claflin, *phys. stat. sol. (b)* **241,** 624–629 (2004).
[8] H. Ohta, M. Orita, M. Hirano, *J. Appl. Phys.* **89,** 5720 (2001).
[9] H. Hosono, H. Ohta, K. Hayashi, M. Orita, M. Hirano, *J. Cryst. Growth* **237–239,** 496 (2002).
[10] M. A. Brusatori, P. R. van Tassel, *Biosensors Bioelectronics* **18,** 1269–1274 (2003).
[11] D. S. Ginley, C. Bright, *MRS Bull.* **25,** 15 (2000).
[12] C. Q. Granqvist, A. Hultåker, *Thin Solid Films* **411,** 1 (2002).
[13] N. Adányi, E. Németh, A. Halász, I. Szendrő, M. Váradi, *Anal. Chim. Acta.* **573–574,** 41 (2006).
[14] N. Adányi, M. Váradi, N. Kim, I. Szendrő, *Current Appl. Phys.* **6,** 279 (2006).

Unauthenticated | Downloaded 06/25/24 06:06 PM UTC